




# Polycomb repressor complex 2 suppresses interferon-responsive MHC-II expression in melanoma cells and is associated with anti-PD-1 resistance

Jamaal L James,<sup>1</sup> Brandie C Taylor <sup>1</sup>, Margaret L Axelrod,<sup>2</sup> Xiaopeng Sun,<sup>1</sup> Lindsey N Guerin,<sup>3</sup> Paula I Gonzalez-Ericsson,<sup>1,4</sup> Yu Wang,<sup>5</sup> Violeta Sanchez,<sup>1</sup> Catherine C Fahey <sup>1,6</sup>, Melinda E Sanders,<sup>4,7</sup> Yaomin Xu,<sup>5</sup> Emily Hodges,<sup>3,8</sup> Douglas B Johnson,<sup>1</sup> Justin M Balko <sup>1,4</sup>

**To cite:** James JL, Taylor BC, Axelrod ML, *et al.* Polycomb repressor complex 2 suppresses interferon-responsive MHC-II expression in melanoma cells and is associated with anti-PD-1 resistance. *Journal for ImmunoTherapy of Cancer* 2023;**11**:e007736. doi:10.1136/jitc-2023-007736

JLJ and BCT are joint first authors.

Accepted 17 October 2023



© Author(s) (or their employer(s)) 2023. Re-use permitted under CC BY-NC. No commercial re-use. See rights and permissions. Published by BMJ.

For numbered affiliations see end of article.

## Correspondence to

Dr Justin M Balko;  
justin.balko@umc.org

## ABSTRACT

**Background** Despite the remarkable success of immunotherapy in treating melanoma, understanding of the underlying mechanisms of resistance remains limited. Emerging evidence suggests that upregulation of tumor-specific major histocompatibility complex-II (tsMHC-II) serves as a predictive marker for the response to anti-programmed death-1 (PD-1)/programmed death ligand 1 (PD-L1) therapy in various cancer types. The genetic and epigenetic pathways modulating tsMHC-II expression remain incompletely characterized. Here, we provide evidence that polycomb repressive complex 2 (PRC2)/EZH2 signaling and resulting H3K27 hypermethylation suppresses tsMHC-II.

**Methods** RNA sequencing data from tumor biopsies from patients with cutaneous melanoma treated with or without anti-PD-1, targeted inhibition assays, and assays for transposase-accessible chromatin with sequencing were used to observe the relationship between EZH2 inhibition and interferon (IFN)- $\gamma$  inducibility within the MHC-II pathway.

**Results** We find that increased EZH2 pathway messenger RNA (mRNA) expression correlates with reduced mRNA expression of both presentation and T-cell genes. Notably, targeted inhibition assays revealed that inhibition of EZH2 influences the expression dynamics and inducibility of the MHC-II pathway following IFN- $\gamma$  stimulation. Additionally, our analysis of patients with metastatic melanoma revealed a significant inverse association between PRC2-related gene expression and response to anti-PD-1 therapy.

**Conclusions** Collectively, our findings demonstrate that EZH2 inhibition leads to enhanced MHC-II expression potentially resulting from improved chromatin accessibility at *C/ITA*, the master regulator of MHC-II. These insights shed light on the molecular mechanisms involved in tsMHC-II suppression and highlight the potential of targeting EZH2 as a therapeutic strategy to improve immunotherapy efficacy.

## BACKGROUND

Immune checkpoint inhibition (ICI) has transformed the landscape of advanced

## WHAT IS ALREADY KNOWN ON THIS TOPIC

⇒ Several studies conducted on murine and patient populations have demonstrated the clinical advantages of major histocompatibility complex-II (MHC-II) expression and its crucial role in responding to immunotherapy. Further, it has been shown that MHC-II may be epigenetically regulated.

## WHAT THIS STUDY ADDS

⇒ This study identifies polycomb repressive complex 2 as a mediator of interferon-responsive MHC-II induction in melanoma cells and establishes a link between this pathway and tumor inflammation. Moreover, we independently identified and validated EZH2 as a mediator of MHC-II proficiency and demonstrated broader connections to immunologic phenotype in tumors, clinical outcome, and potential for therapeutic intervention.

## HOW THIS STUDY MIGHT AFFECT RESEARCH, PRACTICE OR POLICY

⇒ The findings of our study suggest that epigenetic inhibitors, such as Food and Drug Administration approved EZH2, could be employed to counter resistance to immunotherapy, in part by reinstating MHC-II expression.

melanoma therapy. Monoclonal antibodies that block the interaction between programmed death-1 (PD-1) and its ligand (PD-L1) have delivered impressive results compared with the previous standard-of-care treatments. Despite the success of ICI, durable remission only occurs in approximately 30–50% of patients with melanoma.<sup>1</sup> Resistance to ICI remains poorly understood, and currently, no reliable therapeutic strategies exist to overcome either form of resistance.<sup>2</sup> Several factors have been linked to resistance to ICI therapy, including low tumor immunogenicity (eg, low tumor mutational

burden), the presence of immune-suppressive cells within the tumor microenvironment (eg, regulatory T cells and myeloid-derived suppressor cells), and modifications to the antigen presentation pathway (eg, genetic and epigenetic changes to major histocompatibility complexes-I and -II (MHC-I and MHC-II)).<sup>3-8</sup> Tumor cells can downregulate antigen presentation machinery to avoid recognition by cytotoxic CD8+T cells<sup>2</sup>. Loss of MHC-I and MHC-II have been linked to immunotherapy resistance, metastatic progression, and decreased progression-free survival.<sup>8-10</sup> Our group and others have shown that tumor-specific MHC-II expression is a clinically valid positive predictive biomarker of response to anti-PD-1 and anti-PD-L1 therapies in melanoma<sup>10-12</sup> and in other cancers.<sup>13,14</sup> The MHC-II biomarker is now being included as an integrated marker in several upcoming phase III clinical trials. Furthermore, MHC-II expression on tumor cells has been suggested to directly prime CD4+T cells, resulting in enhanced tumor immunity.<sup>15,16</sup> Understanding molecular regulators of MHC-II will be critical in identifying potential targets for drug combinations to counter the immuno-evasive mechanisms underlying anti-PD-1 resistance.

Class II major histocompatibility complex transactivator II (*CIITA*) is the main regulator of the MHC-II pathway and has four known transcriptional promoters that are each epigenetically regulated in a cell type-specific manner.<sup>17</sup> Previous work has shown that decreased expression of enhancer of zeste 2 polycomb repressive complex 2 subunit (EZH2) results in increased MHC-II gene expression.<sup>18</sup> EZH2 is a histone methyltransferase that binds to the *CIITA* locus and catalyzes the histone trimethylation of histone H3 lysine 27 (H3K27me3). It acts as the catalytic subunit of polycomb repressive complex 2 (PRC2).<sup>19</sup> H3K27me3 can be found both at the interferon-gamma (IFN- $\gamma$ )-inducible promoter region and other regulatory regions influencing *CIITA* transcription.<sup>20,21</sup> EZH2 and the PRC2 complex are now clinically targetable,<sup>19</sup> and considering MHC-II expression is a clinically valid biomarker (with potential functional relevance) for immunotherapy response, we sought to further elucidate the relationship between tumor-specific MHC-II suppression and the PRC2 complex in melanoma.

This study explores EZH2 as a target to upregulate MHC-II expression on tumor cells, reinvigorating anti-tumor T cells and overcoming anti-PD-1 resistance through combination therapy. Using publicly available RNA sequencing data from tumor biopsies from patients with cutaneous melanoma, we established a correlative relationship between high expression of PRC2 genes and low expression of both antigen presentation and T-cell genes. Targeted inhibition assays were used to observe the relationship between EZH2 inhibition and IFN- $\gamma$  inducibility within the MHC-II pathway. Additionally, these studies suggested EZH2 inhibition was capable of priming MHC-II-deficient melanoma cell lines for IFN- $\gamma$ -driven MHC-II expression. Assays for transposase-accessible chromatin with sequencing (ATAC-seq) showed that

EZH2 inhibition led to open chromatin at the IFN- $\gamma$ -inducible promoter IV of the *CIITA* gene (*CIITA*-pIV) in MHC-II-deficient cells resulting in IFN- $\gamma$ -driven MHC-II expression. Finally, RNA sequencing data from tumor biopsies of anti-PD-1-treated metastatic melanoma patients showed a correlation between PRC2-related gene expression and patient response to anti-PD-1. These findings provide preclinical data and rationale for using combination therapies involving EZH2 inhibition to overcome anti-PD-1 resistance.

## METHODS

### Clinical samples

All patients provided informed written consent on institutional review board (IRB) approved protocols (Vanderbilt IRB # 030220 and 100178). Clinical samples were collected based on availability from tumor biopsies or resections and analyzed by RNA sequencing and immunohistochemistry as previously described.<sup>11</sup>

RNA isolation: 10  $\mu$ m formalin-fixed paraffin-embedded (FFPE) tumor sections were used for RNA purification. All FFPE blocks were screened by H&E by a research pathologist. Blocks containing at least 20% tumor cellularity were sectioned directly into Eppendorf tubes, whereas those containing less than 20% tumor cellularity were macrodissected with an RNAase-free sterile razor on uncharged glass slides to enrich at least 20% tumor cellularity. RNA was purified using the Maxwell 16 automated workstation (Promega) and the LEV FFPE RNA Tissue Kit (Promega). RNA concentration was determined by spectrophotometry (NanoDrop 2000, Thermo Fisher Scientific). Total RNA quality was assessed using the 2200 TapeStation (Agilent). RNA was sequenced at the Vanderbilt Technologies for Advanced Genomics (VANTAGE) as previously described.<sup>11</sup>

### The Cancer Genome Atlas transcriptional analysis

The melanoma gene expression data set was generated by The Cancer Genome Atlas (TCGA) Research Network (<https://www.cancer.gov/tcga>) and accessed using cBioPortal.<sup>22,23</sup> Z-score normalized gene expression data was downloaded from cBioPortal. Genes were manually selected based on pathways of interest. Hierarchical clustering (k=3) was performed based on gene expression in the R package ComplexHeatmap.<sup>24</sup> Z-scored gene expression was plotted according to hierarchical clustering groups. Statistical comparisons were done using Kruskal-Wallis test with post hoc Dunn tests. Box plots show the median, first and third quartiles. The whiskers extend to the maxima and minima but no further than 1.5 times the IQR.

### Flow cytometry

Flow cytometry was performed on an Attune NxT Flow Cytometer (Thermo Fisher). Cells were washed in phosphate-buffered saline (PBS) and harvested with Accutase (EMD Millipore, #SCR005) for 10 min at

room temperature. Detached cells were washed once in a staining buffer (PBS+1% fetal bovine serum [FBS]) and incubated with Zombie Violet Fixable Viability Dye (BioLegend 423144) at room temperature for 15 min in the dark. Cells were washed once and stained with the following antibodies at 4°C for 25 min in the dark: PD-L1-APC (BioLegend Clone 29E.2A3, 1:400), HLA-A,B,C-Alexa Fluor488 (BioLegend Clone W6/32, 1:200), and HLA-DR-PE/Cy7 (BioLegend Clone L243, 1:200). All data were analyzed using FlowJo software.

### Immunoblotting

Cell cultures were washed with ice cold 1× PBS and harvested using in 1× radioimmunoprecipitation assay buffer (RIPA) buffer (0.1% SDS detergent, 50 mM Tris pH 7.4, 150 mM NaCl, 1.0% NP-40, 0.5% deoxycholic acid, 1 mM EDTA, 1 mM EGTA, 5 mM sodium pyrophosphate, 50 mM NaF, 10 mM β-glycerophosphate) supplemented with phosphatase inhibitors (PhosSTOP, Roche) and protease inhibitors (cOmplete Protease Inhibitor Cocktail, Roche). To extract whole cell protein lysates, contents were scraped from the cell culture plates and incubated on ice for 30 min before centrifugation at 13,000×g for 15 min at 4°C. Protein lysates were quantitated for protein concentration using a BCA assay (Thermo). Samples were separated on NuPAGE 4–12% Bis-Tris gels (Invitrogen) and transferred to nitrocellulose membranes. Membranes were blocked with 5% non-fat dry milk or 5% bovine serum albumin (BSA) in tris-buffered saline supplemented with 0.1% Tween-20 for 1 hour at room temperature. Membranes were then incubated in the appropriate blocking buffer overnight at 4°C using antibodies to the indicated targets. Following incubation with the proper horseradish peroxidase-conjugated secondary antibodies, proteins were visualized using an enhanced chemiluminescence detection system (Thermo). This study was completed using antibodies specific for the following targets: GAPDH (clone 0411; sc-47724, Santa Cruz), EZH2 (clone D2C9; #5246, Cell Signaling), Tri-Methyl (K27) Histone H3 (clone C36B11; #9733, Cell Signaling), PD-L1 (clone E1L3N; #13864, Cell Signaling), HLA-A,B,C (clone LY5.1; #sc-3147, Santa Cruz), and HLA-DR (clone TAL 1B5; #sc-53319, Santa Cruz).

### siRNA transfections

Reverse transfection was carried out in 6-well culture plates (Corning) using 2.5 μL of 20 μM *EZH2*-targeting siRNA stock (Thermo Fisher Scientific) and 5 μL of DharmaFECT I transfection reagent (Dharmacon) in 500 μL Opti-MEM (Gibco). This was combined with 1×10<sup>5</sup> cells suspended in 2 mL of media. After 48 hours, cells were harvested and re-seeded at 1–2×10<sup>5</sup> cells per well and treated with IFN-γ for 24–48 hours and harvested for protein, messenger RNA (mRNA), or single cell suspensions 48 hours after transfection.

### Cell lines and treatment

Human melanoma cancer cell lines A375 (DMEM+10% FBS), SKMEL-5 (DMEM+10% FBS), SKMEL-28 (DMEM+10% FBS), COLO829 (RPMI+10% FBS), MeWo (MEM+10% FBS), SKMEL-1 (MEM+10% FBS), and CHL-1 (DMEM+10% FBS) were obtained from American Type Culture Collection. All cells were routinely tested for *Mycoplasma* contamination. For in vitro experiments involving EZH2 targeting, seeded cells were pretreated with 5 μM GSK343 (Selleckchem) or 5 μM tazemetostat (Selleckchem) for 3 days before the addition of IFN-γ for 24–48 hours.

### qPCR analysis

RNA was analyzed for concentration by a NanoDrop 2000 (Thermo Fisher Scientific) before complementary DNA (cDNA) synthesis using SensiFAST cDNA Synthesis Kit (Bioline, Meridian Bioscience, Catalog BIO-65054) with 1 μg of RNA per sample. cDNA and SsoAdvanced Universal SYBR Green Supermix (Bio-Rad, Catalog 1725270) were then combined with target-specific primers on a CFX96 Touch Real-Time PCR Detection System (Bio-Rad). Three technical replicates were used for each reaction. GAPDH was used as the housekeeping gene. Primers used were: *EZH2*: F: 5'-GACCTCTGTCTTACTTGTGGAGC-3' R: 5'-CGTCAGATGGTGCCAGCAATAG-3'; *CIITA*: F: 5'-CTACTTCAGGCAGCAGAGGAGA-3' R: 5'-GCTGTGTCTTCCGAGGAAGTTC-3'; *CD74*: F: 5'-AAGCCTGTGAGCAAGATGCGCA-3' R: 5'-AGCAGGTGCATCACATGGTCCT-3'; *GAPDH* F: 5'-TGCACCACCAACTGCTTAGC-3' R: 5'-GGCATGGACTGTGGTCATGAG-3'; *CIITA*-pIV (promoter IV): F: 5'-AGGGAGAGGCCACCAGCAG-3' R: 5'-GAACTGGTTCGAGTTGATG-3'; *CIITA*-pIII (promoter III): F: 5'-GCCCTGCTGGGTCCTACCTG-3' R: 5'-GAACTGGTTCGAGTTGATG-3'

### Assays for transposase-accessible chromatin with sequencing

ATAC-seq libraries were prepared as previously reported with minor modifications (Buenrostro *et al*, 2013). Briefly, 100,000 CHL1 cells of each sample group were harvested. Cells were processed as described with the resulting nuclei pellet being resuspended in 95 mL transposition reaction mix (10 mM Tris-HCl pH 7.5, 5 mM MgCl<sub>2</sub>, 10% dimethylformamide) by pipetting up/down with a 200 μL micropipette tip five times. 5 mL of pre-assembled Tn5 transposome with standard ATAC adapters (included below) was added. Tubes were gently agitated and incubated at 37°C, 1 hour, 700 RPM in an Eppendorf ThermoMixer. ATAC reactions were purified according to manufacturer instructions in a DNA Clean and Concentrator-5 kit (Zymo) and eluted in 25 mL nuclease-free water. Eluted fragments were amplified and barcoded in 50 μL PCR reactions (25 μL 2× NEBNext High-Fidelity PCR Master Mix, 20 μL eluted ATAC DNA, 2.5 μL 10 mM i5 index primer, 2.5 μL 10 mM i7 index primer). Post-amplification PCR reactions were size selected using SPRIselect (Beckman Coulter) according to the



manufacturer's instructions for right side size selection at a ratio of 0.6×. Preliminary library analysis for concentration and size distribution was performed using an Agilent 2200 TapeStation with a D5000 tape. Primer sequences are as follows: Tn5MEREV oligo (5'→3'): 5Phos/CTGTCTCTTATACACATCT; Tn51 oligo (5'→3'): TCGT CGGCAGCGTCAGATGTGTATAAGAGACAG; Tn5\_2\_ME\_Comp oligo (5'→3'): TCTCGTGGGCTCGGAG ATGTGTATAAGAGACAG

### Statistical analysis

Statistics were performed in GraphPad Prism or R (www.r-project.org). In data with two groups, two-sample t-tests were used, or Mann-Whitney U tests when indicated. For analyses with >2 groups, significant differences were determined by analysis of variance with a Tukey's post hoc test adjustment for multiple comparisons. For all multiple comparisons, statistical significance is noted by \* $p < 0.05$ ; \*\* $p < 0.01$ , and \*\*\* $p < 0.001$ . A  $p$  value of  $< 0.05$  was considered statistically significant. Bar graphs show mean±SEM, unless otherwise stated in the figure legend.

## RESULTS

### PRC2-enriched tumors correlate with low gene expression patterns of antigen presentation and T-cell infiltration

To determine the relationship between genes encoding PRC2 subunits and T-cell genes in melanoma tumors, hierarchical clustering was performed using a targeted subset of RNA sequencing data (comprising genes associated with PRC2, class I antigen presentation, class II antigen presentation, T-cell activation and T-cell suppression) from 363 patient with melanoma tumors in the TCGA.<sup>10</sup> Three clusters were identified as “PRC2<sup>hi</sup>”, “T cell<sup>hi</sup>”, or “Intermediate”, which separated tumors by the relative expression of the indicated genes involved in either PRC2 activity or T-cell response (figure 1A). Substantially lower expression levels of T-cell activation/suppression genes and antigen presentation genes were found in PRC2<sup>hi</sup> tumors, indicating an inverse and potentially antagonistic relationship between PRC2 activity and antitumor T-cell responses.

The identified clusters were further used to assess the relationship between T-cell response genes and PRC2-related genes. PRC2-directed histone methylation requires both the catalytic activity of EZH2, as well as the targeting of PRC2 to specific genes by Jumoni and AT-rich interaction domain-containing protein (JARID2).<sup>19</sup> Therefore, *EZH2* and *JARID2* were chosen to confirm the significance of PRC2 in the altered gene expression patterns among the three patient clusters. Both *EZH2* and *JARID2* were expressed at significantly reduced levels in T cell<sup>hi</sup> and Intermediate tumors compared with PRC2<sup>hi</sup> tumors (figure 1B).

In agreement with previous work,<sup>18</sup> *CIITA* expression was significantly decreased in both PRC2<sup>hi</sup> and Intermediate tumors compared with T cell<sup>hi</sup> tumors (figure 1B), suggesting that antigen presentation by MHC-II could

be suppressed at the mRNA level in tumors with highly expressed PRC2 genes. This is further supported by high mRNA expression levels among conventional T-cell-related genes cells markers, including total T cells (*CD3E*), T helper cells (*CD4*), and cytotoxic T cells (*CD8A*), in the T cell<sup>hi</sup> cluster but significantly reduced in the PRC2<sup>hi</sup> cluster (figure 1A,B). These data suggest that the overexpression of PRC2 genes is associated with a reduced intertumoral T-cell presence and may antagonize the potential for antigen presentation within the tumor microenvironment.

### HLA-DR-negative melanoma cells have high expression of PRC2-related genes

As the TCGA completed RNA sequencing on whole tumor samples, the data set is representative of all cell types commonly found within the tumor microenvironment, including tumor cells, endothelial cells, normal epithelium, and immune cells. To examine the relationship of *EZH2* and MHC-II genes specifically in tumor cells, real-time quantitative PCR was completed in various melanoma cell lines. Human melanoma cell lines express varying levels of HLA-DR, an MHC-II surface receptor, at baseline and in response to IFN- $\gamma$  stimulation, indicating differences in MHC-II regulation.<sup>10</sup> Therefore, to examine differences in MHC-II expression and regulation, a panel of melanoma cells were stimulated with IFN- $\gamma$  for 24 hours. Within the panel, three cell lines—A375, COLO829, and SKMEL-5 demonstrated upregulated human leukocyte antigen-DR (HLA-DR) expression (MHC-II-proficient), while MeWo, SKMEL-1, and CHL-1 remained HLA-DR-negative (MHC-II-deficient) (figure 1C). Among the panel of MHC-II proficient and deficient cells, mRNA expression patterns mirrored trends within the patient cohort, showing an inverse correlation in expression between *EZH2/JARID2* expression and *CIITA/CD74* expression (figure 1D).

### Pharmacological or genetic inhibition of EZH2 in MHC-II proficient cell lines has modest overall effect on MHC-II expression

To examine the effect of *EZH2* loss on MHC-II expression, we first used siRNA to knockdown *EZH2* in three MHC-II proficient cell lines. *EZH2* knockdown (most notable in COLO829), led to modest increases in mRNA expression in both *CIITA* and *CD74*, a representative MHC-II-associated gene (figure 2A). Modest and variable increases in total MHC-II protein expression by immunoblot (figure 2B) and cell-surface MHC-II expression by flow cytometry (figure 2C) were observed, primarily at earlier (24 hours) time points. We next tested the effect of pharmacologic and genetic, as the intrinsic effects of small molecule inhibition are more immediate and controllable. A375 and SKMEL-5 were treated with the *EZH2* inhibitors, GSK343 or tazemetostat, followed by IFN- $\gamma$  stimulation for 0, 24, or 48 hours. In contrast to genetic inhibition, pharmacologic inhibition of *EZH2* function led to more appreciable changes in MHC-II



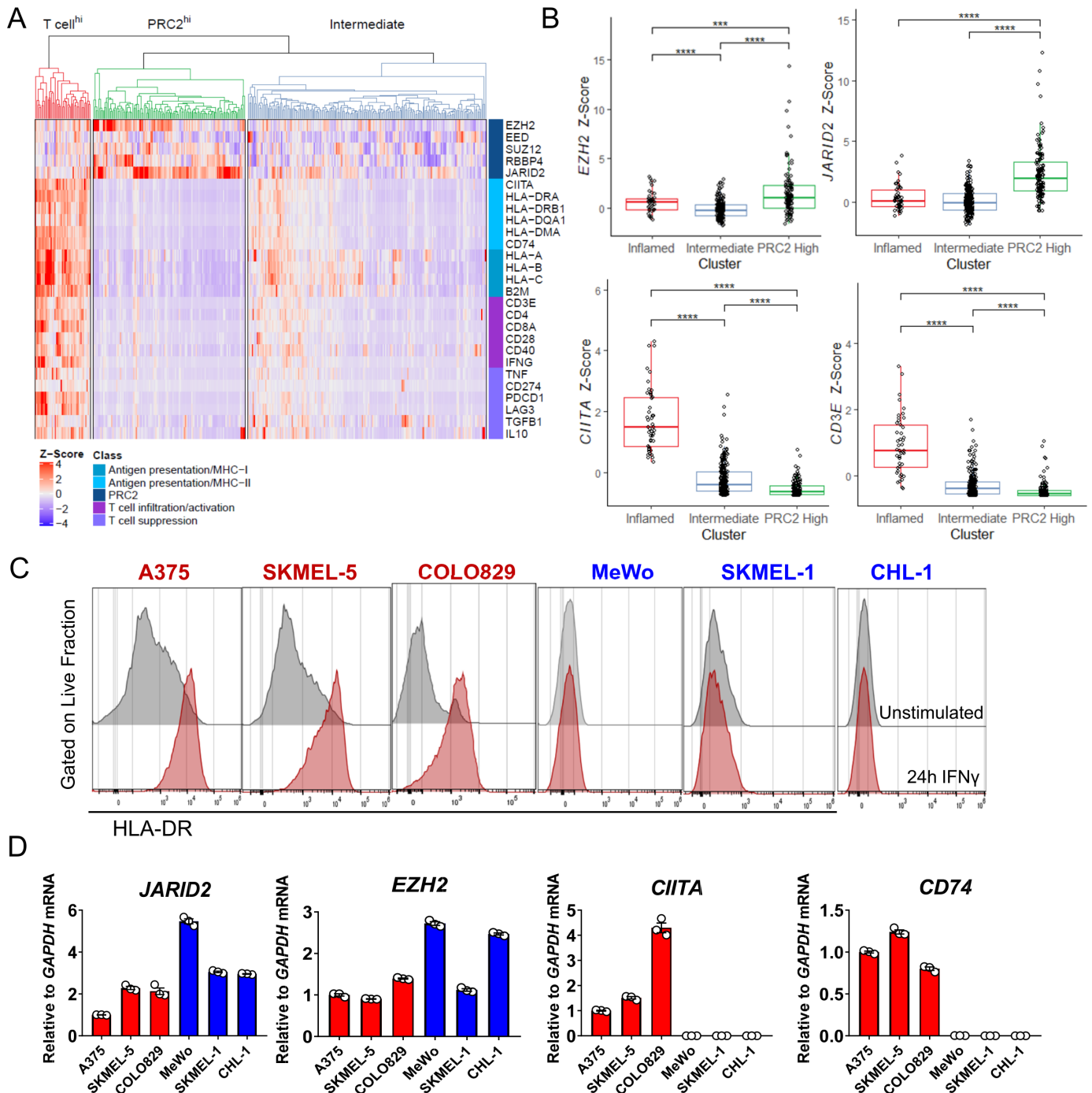


**Figure 1** High expression of PRC2 genes correlates with low expression of tumor-specific MHC class II genes. (A) Cluster analysis was performed using z-scores calculated from RNA sequencing expression data of patient with melanoma tumors gathered from The Cancer Genome Atlas. (B) mRNA expression of PRC2 genes (*EZH2* and *JARID2*) and T-cell genes (*CD3E*, *CD4*, *CD8A*) across T cell<sup>hi</sup> (red boxes), Intermediate (blue boxes), and PRC2<sup>hi</sup> (green boxes) patient clusters. Box plots show the median, first and third quartiles. The whiskers extend to the maxima and minima but no further than 1.5 times the IQR. Data were analyzed by analysis of variance followed by a Tukey's post hoc test. \*\*\*p<0.001; \*\*\*\*p<0.0001. (C) Flow cytometry histograms representing live fractions of interferon- $\gamma$ -stimulated (red histograms) human melanoma cell lines compared with unstimulated controls (gray histograms). Following staining with a live-dead dye, cells were labeled with fluorophore-conjugated HLA-DR antibodies. (D) qPCR analysis of human melanoma cell lines characterized for mRNA expression of the indicated genes of interest relative to GAPDH mRNA expression values for each cell line. Values were calculated as fold expression relative to A375 cells. CIITA, class II major histocompatibility complex transactivator II; EZH2, enhancer of zeste 2 polycomb repressive complex 2 subunit; HLA-DR, human leukocyte antigen-DR; JARID2, Jumoni and AT-rich interaction domain-containing protein; MHC, major histocompatibility complexes; mRNA, messenger RNA; PRC2, polycomb repressive complex 2; qPCR, quantitative polymerase chain reaction.

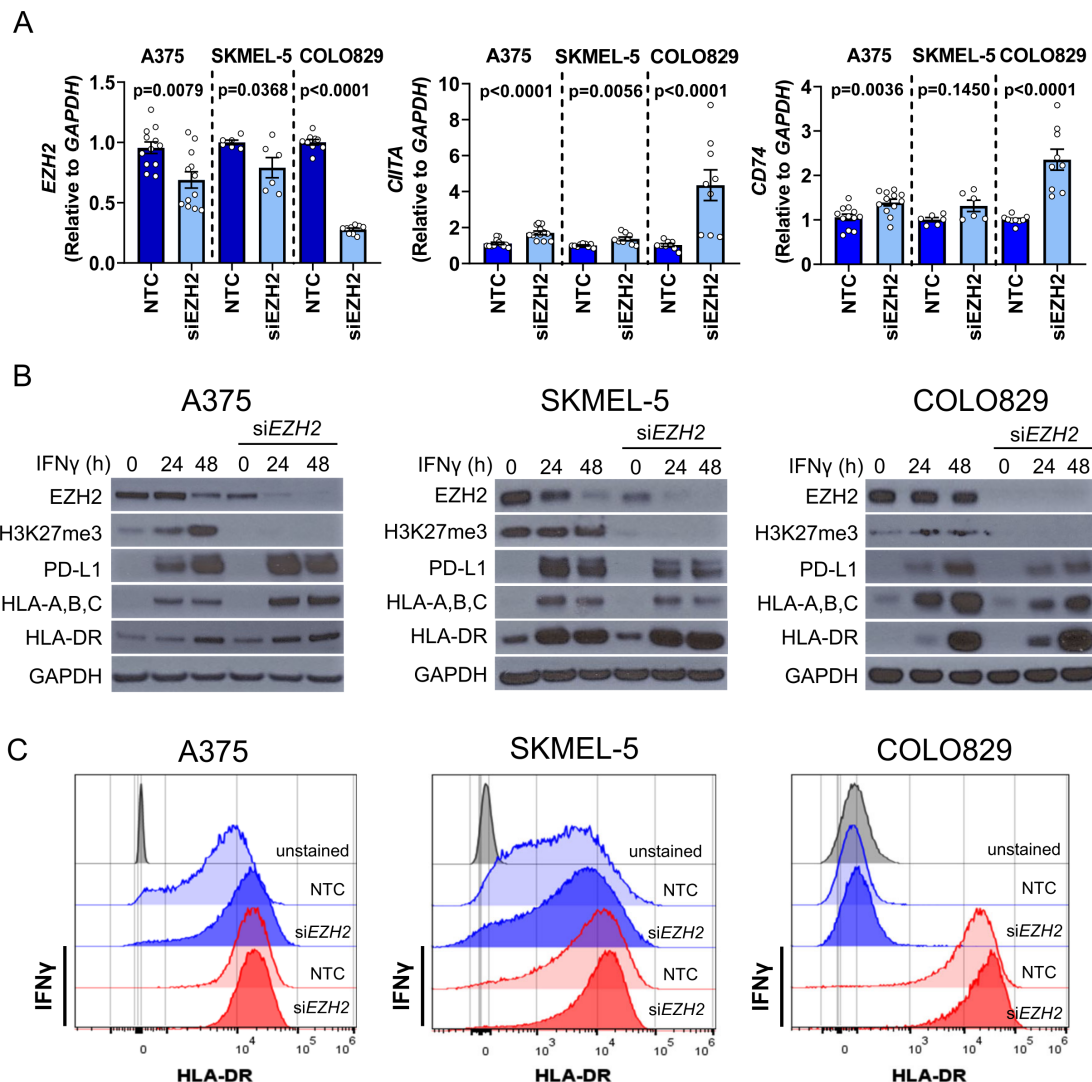


**Figure 2** *EZH2* knockdown moderately increases expression of MHC class II. (A) *EZH2*, *CIITA*, and *CD74* mRNA expression in MHC-II-proficient cell lines after transfection with *EZH2* siRNA or to non-targeting control (NTC). Values were normalized to *GAPDH* mRNA and calculated as fold expression values relative NTC siRNA. The data shown represents combined technical replicates derived from three to four independent experiments. (B) after 24–48 hours IFN- $\gamma$  stimulation, whole cell protein lysates were extracted from siRNA-transfected MHC-II-proficient cell lines probed with monoclonal antibodies specific for the indicated proteins. Lysates were normalized to *GAPDH* expression. Data represent one of two experimental replicates. (C) Flow cytometry analysis of MHC-II-proficient cell lines transfected with siEZH2 or NTC and stained with fluorophore-conjugated HLA-DR antibodies. The histograms shown in C represent one of at least three independent experiments. *CIITA*, class II major histocompatibility complex transactivator II; *EZH2*, enhancer of zeste 2 polycomb repressive complex 2 subunit; IFN, interferon; HLA-DR, human leukocyte antigen-DR; MHC, major histocompatibility complexes; mRNA, messenger RNA.

gene and protein expression, both at baseline and after IFN- $\gamma$  stimulation (figure 3A–C), although changes at the transcriptional level were more variable (figure 3D,E). Thus, in melanoma cells that are already MHC-II proficient, *EZH2* inhibition has generally modest effects on further increasing MHC-II expression.

#### **EZH2 inhibition converts MHC-II-deficient melanoma cells to proficient**

Previous studies in multiple cancer types have implicated *EZH2* in the genetic repression of various IFN- $\gamma$  targets, including *CD274/PD-L1*, *HLA-A*, *HLA-B*, and *IRF-1*.<sup>25, 26</sup> Thus, we next hypothesized that the MHC-II-deficient phenotype may be reflective of broader

epigenetic defects in inflammatory signaling, and *EZH2* inhibition may produce more robust effects in re-wiring IFN responses in MHC-II deficient tumor cells. Surface HLA-DR expression was increased in the MHC-II-deficient cells after IFN- $\gamma$  stimulation in the presence of tazemetostat treatment (figure 4A,B). Protein isolates from these conditions showed IFN- $\gamma$  stimulation alone induced PD-L1 but not HLA-DR, confirming that MHC-II deficiency is not associated with complete disruption in IFN- $\gamma$  response signaling (figure 4C). Both MHC-II and MHC-I expression were enhanced after tazemetostat pretreatment under IFN- $\gamma$ -stimulated conditions (figure 4C; HLA-DR detection by western blot was below the limit of detection in

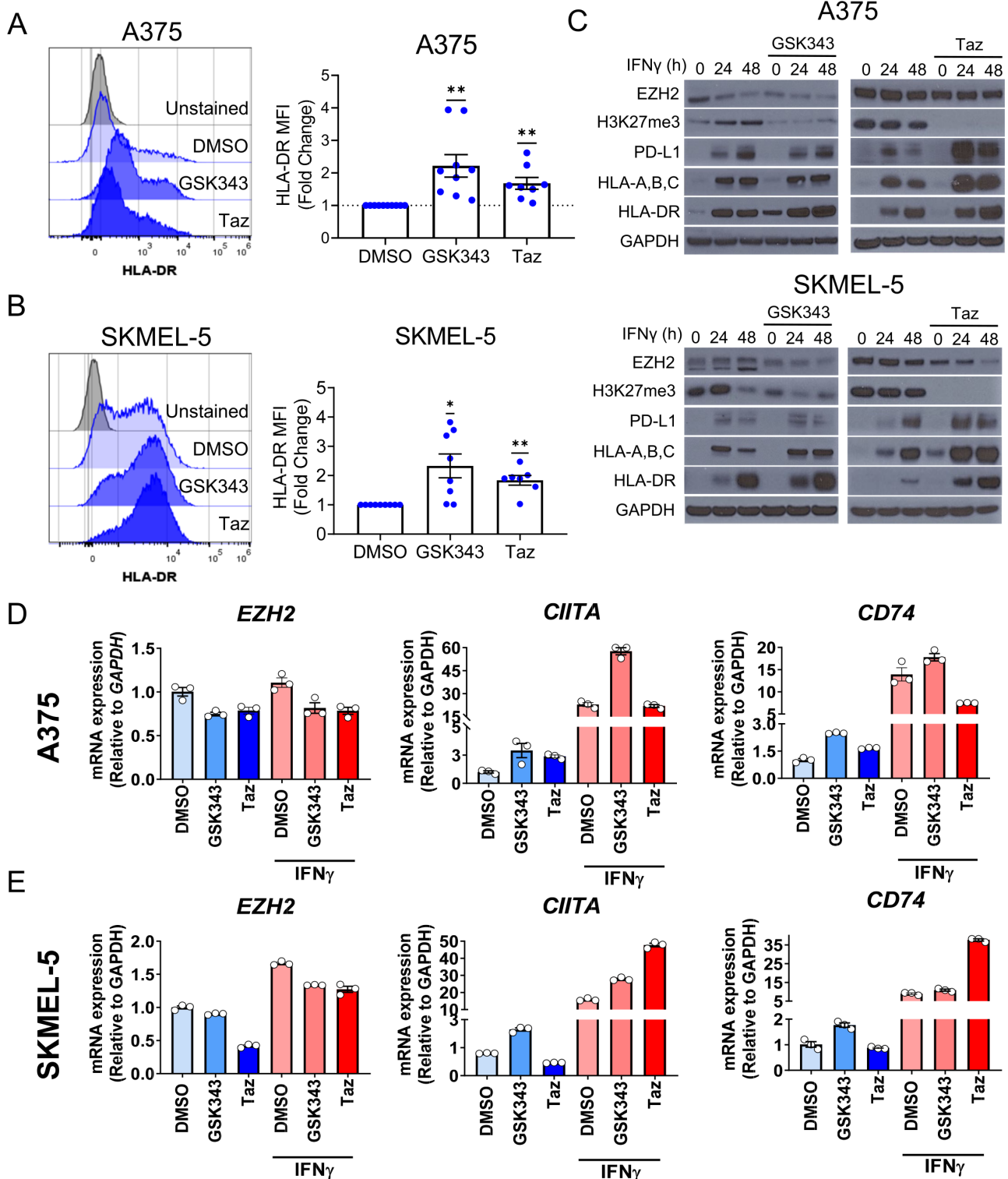


**Figure 3** Pharmacological inhibition of EZH2 upregulates interferon-induced major histocompatibility complexes expression. (A–B) Flow cytometry analysis of A375 and SKMEL-5 cell lines treated with the indicated EZH2 inhibitor for 5 days. Single cell suspensions were stained with fluorophore-conjugated antibodies HLA-DR. \* $p < 0.05$  and \*\* $p < 0.01$ , one-sample t-test against a fold change of 1. (C) After stimulation with IFN- $\gamma$  for 24–48 hours, whole cell protein lysates were extracted from A375, SKMEL-5, and COLO829 cells treated with DMSO or EZH2 inhibitor before being probed for the indicated proteins. Data shown represents three independent experiments. (D–E) Relative expression of EZH2, CIITA, and CD74 mRNA extracted from melanoma cell lines treated with GSK343 or tazemetostat and stimulated with IFN- $\gamma$  for 24–48 hours. Samples were normalized to GAPDH mRNA and calculated as fold expression relative to the DMSO control. CIITA, class II major histocompatibility complex transactivator I; DMSO, dimethyl sulfoxide; EZH2, enhancer of zeste 2 polycomb repressive complex 2 subunit; HLA-DR, human leukocyte antigen-DR; IFN, interferon; MFI, mean fluorescence intensity; mRNA, messenger RNA; PD-L1, programmed death ligand 1.



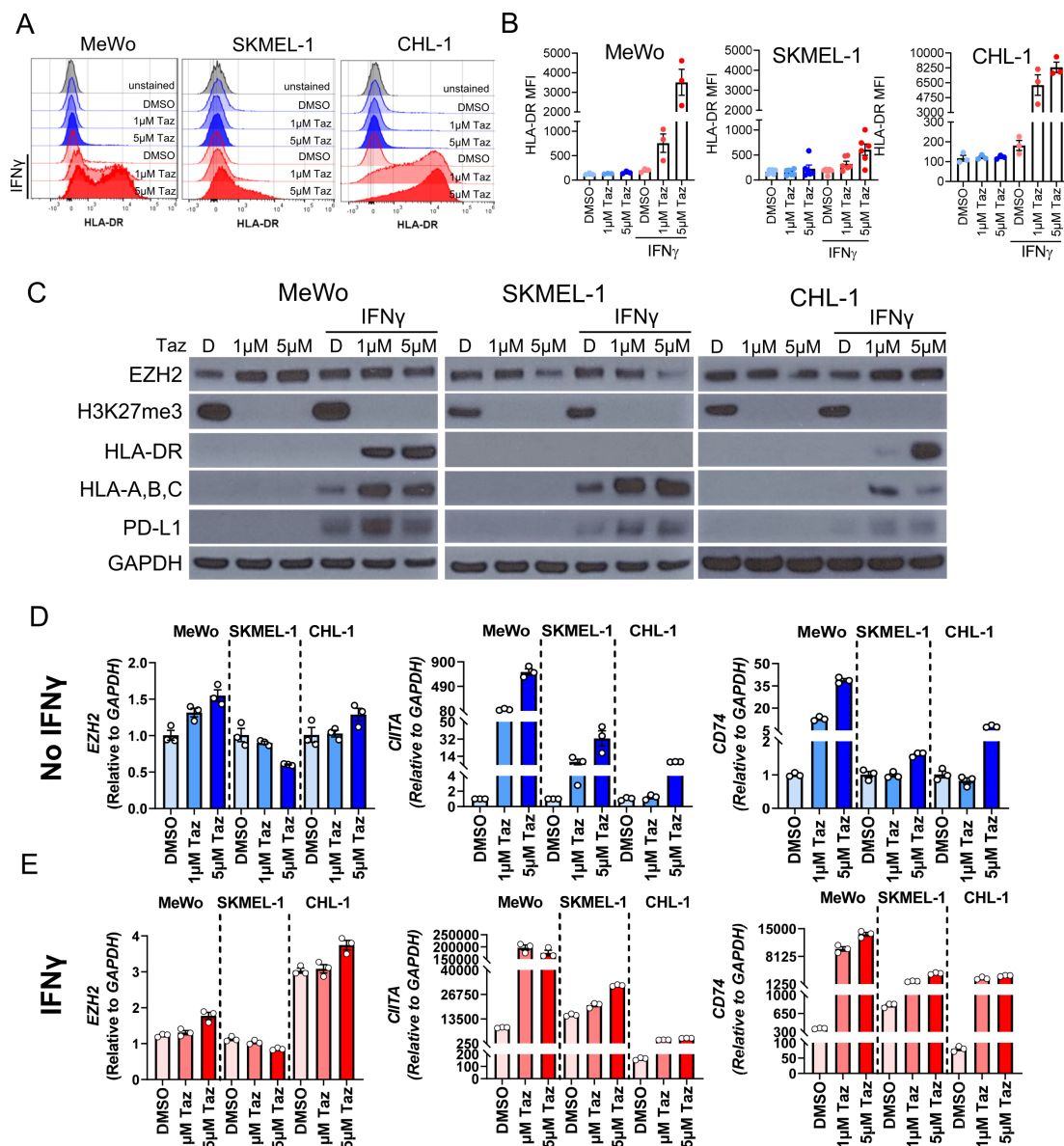


**Figure 4** Tazemetostat reverses major histocompatibility complexes II-specific IFN- $\gamma$  resistance in MeWo, SKMEL-1, and CHL-1 cells. Cells were pretreated with tazemetostat (1  $\mu$ M or 5  $\mu$ M) for 3–4 days and stimulated with IFN- $\gamma$  for 72 hours. (A–B) On harvest, cells were stained with the indicated antibodies and visualized for surface expression using flow cytometry. (C) Western blots using whole cell lysates and probed with antibodies specific for the indicated targets. HLA-DR expression was below the limit of detection for western blot in SKMEL1 (less sensitive than flow cytometry). (D–E) Quantitative real time PCR performed on messenger RNA isolates after tazemetostat treatment and IFN- $\gamma$  stimulation. CIITA, class II major histocompatibility complex transactivator I; DMSO, dimethyl sulfoxide; EZH2, enhancer of zeste 2 polycomb repressive complex 2 subunit; HLA-DR, human leukocyte antigen-DR; IFN, interferon; MFI, mean fluorescence intensity; PD-L1, programmed death ligand 1.

SKMEL-1). Additionally, *CIITA* and *CD74* mRNA expression levels were upregulated at baseline after tazemetostat treatment and became more IFN- $\gamma$ -responsive (figure 4D,E). Overall, tazemetostat-dependent priming (ie, pretreatment) for IFN- $\gamma$ -responsiveness within the MHC-II pathway indicates a mechanism for genetic repression at the MHC-II gene locus, that is, unique from other IFN- $\gamma$  targets (eg, PD-L1)<sup>10</sup> and predominantly controlled by PRC2/EZH2-dependent methyltransferase activity.

#### EZH2 inhibition with tazemetostat leads to chromatin accessibility at multiple regulatory regions across the *CIITA* locus

We next sought to confirm that EZH2 inhibition resulted in direct changes in chromatin accessibility at the *CIITA* locus, the master regulator of MHC-II gene expression. We first examined the locus for sites of particular interest (figure 5A). There are four known *CIITA* promoters; the dendritic cell promoter (pI), an inadequately defined enhancer-like region commonly identified as “pII,” the B-cell promoter (pIII), and the IFN- $\gamma$ -inducible promoter (pIV).<sup>27</sup> EZH2/PRC2-dependent histone trimethylation

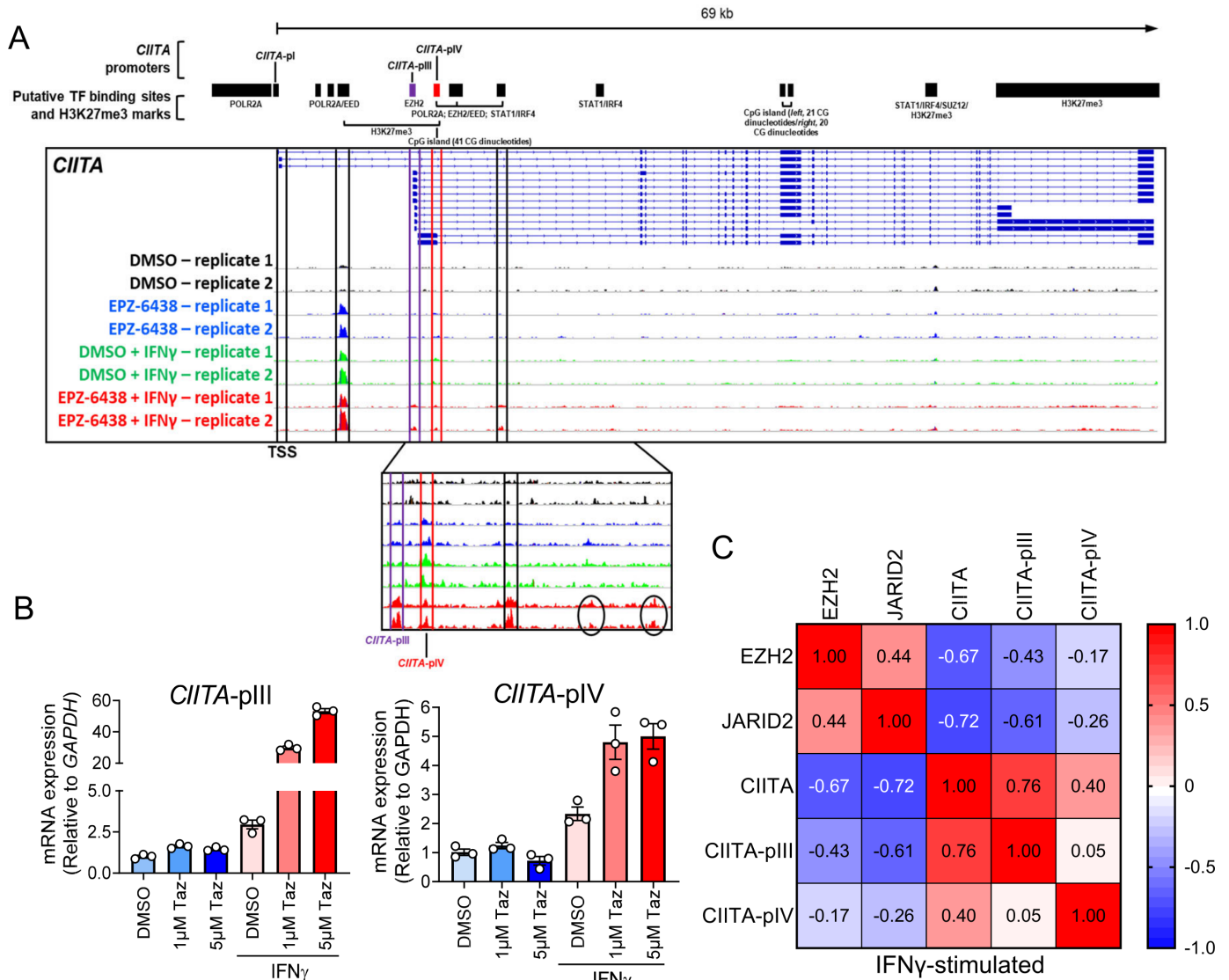


**Figure 5** Tazemetostat treatment exposes accessible chromatin at regions containing putative IRF1 and STAT1 binding motifs in IFN- $\gamma$ -stimulated CHL-1 cells. (A) CHL-1 cells were pretreated for 4 days with tazemetostat before 24 hours stimulation with IFN- $\gamma$ . Cells were harvested and processed for assays for transposase-accessible chromatin with sequencing. Black bars represent predicted target sites for H3K27me3 marks, CpG islands, and promoters driving transcription of the indicated genes, based on the publicly available data from multiple tissue types and conditions in the UCSC database. Putative transcription factor (TF) binding sites for IFN- $\gamma$  signaling (STAT1 and IRF4), based on predictions made using the <https://molotool.autosome.org/> and a permissive p value setting of 0.0005. (B) mRNA expression assessed by qPCR using primers specific for the pIII and pIV 5'UTR. (C) Correlation matrix for qPCR data across seven cell lines (A375, SKMEL5, COLO829, SKMEL28, MEWO, SKMEL1, and CHL1) under interferon-stimulated conditions. CIITA, class II major histocompatibility complex transactivator II; DMSO, dimethyl sulfoxide; EZH2, enhancer of zeste 2 polycomb repressive complex 2 subunit; IFN, interferon; JARID2, Jumoni and AT-rich interaction domain-containing; mRNA, messenger RNA; pIV, promoter IV; qPCR, quantitative polymerase chain reaction; UCSC, University of California, Santa Cruz.

is thought to recruit DNA methyltransferases to specific CpG-rich genomic regions for DNA methylation<sup>19</sup>; therefore, three separate CpG islands were considered in the analysis, including a common CpG island located directly at *CIITA*-pIV. Finally, ENCODE chromatin immunoprecipitation (ChIP)-seq data for acetylated H3K27 and trimethylated H3K4, which function as epigenetic marks of active transcription and putative transcription factor binding sites, were assessed. These targets include IRF1

and STAT1, which are necessary for IFN- $\gamma$ -responsive control of *CIITA* transcription.<sup>28</sup>

We used ATAC-seq in the MHC-II-deficient melanoma cell line CHL-1 to assess the effect of tazemetostat on chromatin accessibility, with our analysis focused on these sites of interest (figure 5A). As expected, pI was inaccessible at baseline and remained inaccessible under all treatment conditions, confirming previous reports of pI having little to no involvement in IFN- $\gamma$ -dependent *CIITA*

transcription.<sup>29</sup> However, the “pII” enhancer, already accessible at baseline, appeared similarly responsive to all treatment conditions, indicating an ability of both IFN- $\gamma$  and tazemetostat to induce activity. Although IFN- $\gamma$  and tazemetostat are capable of inducing “pII” accessibility, open chromatin at “pII” alone is not sufficient for the induction of MHC-II expression as demonstrated by the lack of response in MHC-II deficient lines (figure 3). Similarly, chromatin at pIV opened in response to either tazemetostat or IFN- $\gamma$  as single agents, suggesting that neither “pII” nor pIV are sufficient for MHC-II expression. In contrast, chromatin at pIII and a downstream STAT1/IRF4 site uniquely opened in response to the combination of tazemetostat followed by IFN stimulation, suggesting these sites may cooperate to drive MHC-II expression.

Given the context-specific and cell-specific coordination between activated *CIITA* promoters and enhancers along with previous findings highlighting EZH2-dependent transcriptional repression of *CIITA*-pIV,<sup>30</sup> we measured IFN- $\gamma$ -responsiveness at pIII and pIV in CHL-1 cells treated with tazemetostat. Using *CIITA*-pIII-specific or *CIITA*-pIV-specific primers, quantitative polymerase chain reaction (qPCR) was performed to measure *CIITA* promoter activity by gene expression. While similar patterns in relative expression were present at both pIII and pIV, the combinatorial effect of tazemetostat treatment and IFN- $\gamma$  stimulation resulted in a substantially higher expression enhancement at pIII, consistent with our ATAC-seq data (figure 5B,C). When examining gene expression data across all cell lines under IFN- $\gamma$  stimulation conditions, pIII expression correlated strongly with total *CIITA* expression, and negatively with PRC2 (*JARID2/EZH2*) gene expression (figure 5C).

#### High *JARID2* mRNA expression correlated with low tumor HLA-DR expression and a suboptimal anti-PD-1 response

Previous studies by our laboratory have shown that high tumor HLA-DR expression (>5% of tumor cells) by immunohistochemistry (IHC) predicts anti-PD-1 response in patients with metastatic melanoma.<sup>11</sup> To determine if PRC2 gene expression patterns were directly associated with tumor inflammation, tumor specific MHC-II expression, and clinical response to ICI, we performed RNA sequencing on a series of 64 metastatic melanomas with corresponding immunohistochemical staining for HLA-DR in the tumor compartment. As observed with the TCGA data, high expression of genes encoding PRC2 subunits generally correlated with low expression of T cell and MHC-II antigen presentation genes (figure 6A–C). As we have previously published, an IHC score of 5% cut-off distinguishing high ( $\geq 5\%$ ) versus low ( $\leq 5\%$ ) tumor HLA-DR positivity confirmed a significant association with higher *JARID2* expression in tumor cell-specific MHC-II negative tumors (figure 6D).

Patients in this cohort were treated with ICI treatment single agent pembrolizumab (anti-PD-1) with no prior anti-cytotoxic T-lymphocyte-associated protein 4

(anti-CTLA; ipilimumab) therapies (“Ipi-naïve”; n=25), with prior ipilimumab treatment (“ipi-progression”; n=18), or with combination therapies (n=21). Since these groups have previously been shown to have biological differences (specifically those with prior ipilimumab<sup>31</sup>) we determined whether PRC2 gene expression was associated with clinical response to ICI in each group. Patients were grouped as responders (those with complete response or partial response) or non-responders (stable disease or progressive disease). Patients lacking clinical response to anti-PD-1 therapy demonstrated higher expression of *JARID2*, but only in ipilimumab-naïve patients (figure 6E–G). Thus, there is evidence that high PRC2 expression is associated with MHC-II expression and intrinsic resistance to anti-PD-1 therapy. On analyzing our patient data, we did not observe a significant correlation between EZH2 expression and response to therapy. *JARID2* plays a crucial role in coordinating PRC2 recruitment and stimulating H3K27 methylation activity, which is essential for epigenetic gene silencing. Therefore, we have chosen to present the data as shown to demonstrate the correlation between DNA methylation, patient response, and MHC-II expression

#### DISCUSSION

Tumor specific MHC-II expression has been demonstrated to be a viable clinical predictor of response to anti-PD-1/L1 immunotherapy in a variety of cancer types, including melanoma.<sup>10 12–14 32</sup> It has been well-established that cancer cells demonstrate distinct differences in the ability to upregulate MHC-II, which results in diverse expression patterns.<sup>10 11 32</sup> Prior studies have demonstrated that a cancer cell’s ability to upregulate MHC-II in response to IFN stimulation is a unique property of the cell state,<sup>33</sup> and independent of PD-L1 expression.<sup>10</sup> Both MHC-II/*CIITA* and PD-L1 require JAK/STAT signaling downstream of the IFN receptor. Therefore, this uncoupling of cellular responses may be due to distinct differences in transcription factor presence,<sup>28</sup> or due to changes in the epigenetic state of the cell.<sup>17 27 33 34</sup> Our study suggests the use of epigenetic inhibitors may play a role in overcoming resistance to immunotherapy at least in part by restoring MHC-II expression.

Previous groups have demonstrated that normal epithelial cells<sup>35–37</sup> and other cancer-progenitor cell types, like melanocytes,<sup>38</sup> will express MHC-II under inflammatory conditions, suggesting a non-pathogenic function in immune homeostasis. However, the function of these non-professional antigen presenting cells (non-pAPCs) expressing MHC-II has not been clearly defined. Furthermore, these studies suggest the loss of MHC-II capacity in cancer may be tumor promoting.<sup>39</sup> Another study suggested cancer cells are capable of directly presenting MHC-II antigens to CD4+T cells, which could result in enhanced immunity.<sup>15</sup> Despite these functions, currently there are no well-established mechanisms for self-presentation of MHC-II antigens by non-pAPCs.<sup>40 41</sup>



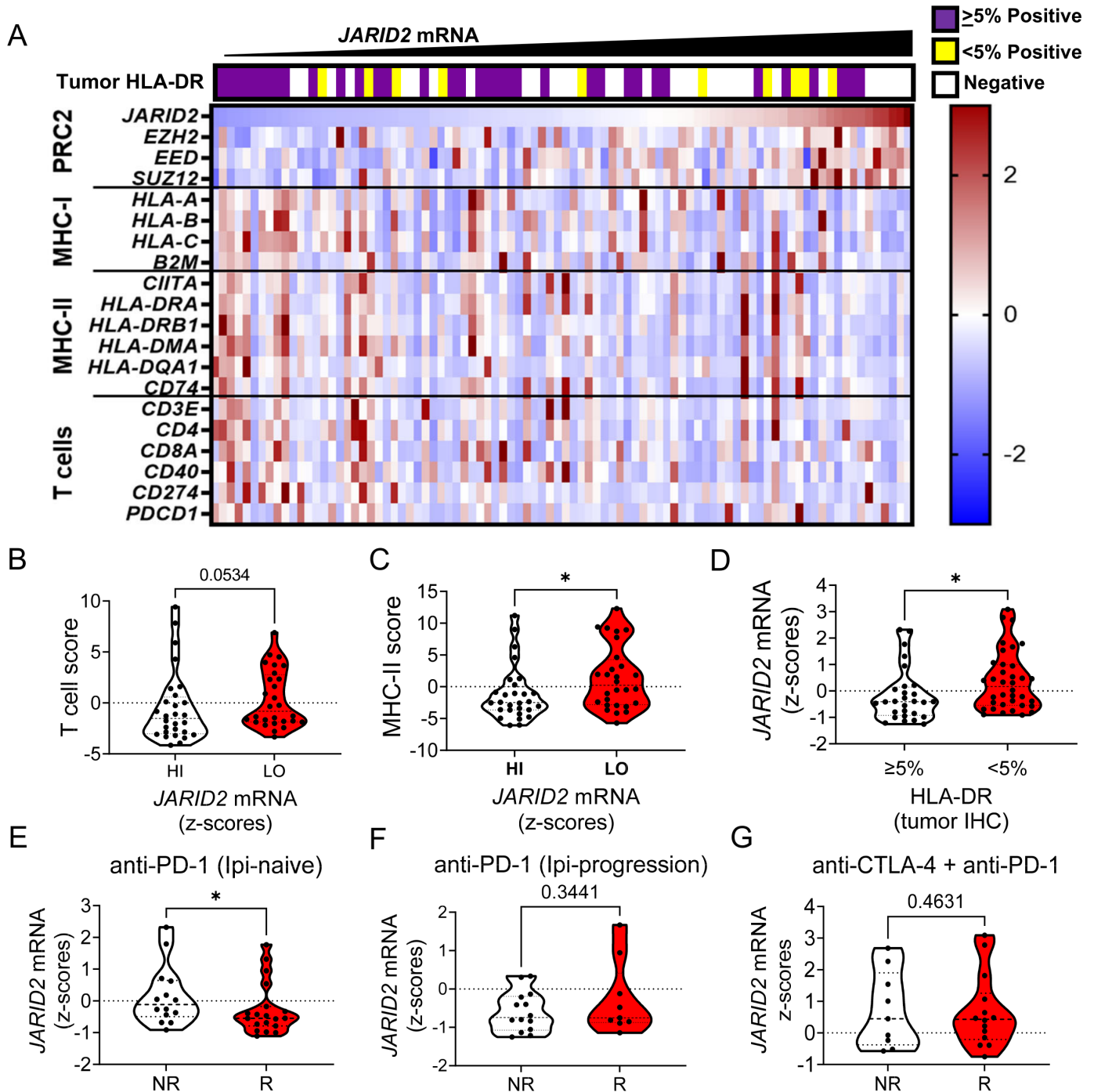


**Figure 6** Anti-PD-1-responsive human metastatic melanoma tumors express lower levels of *JARID2* mRNA compared with non-responders. (A) Heatmap representing human melanoma RNA sequencing z-scores of genes relevant to PRC2, T cells, and antigen presentation by MHC-I and MHC-II. Samples were ordered by increasing *JARID2* mRNA expression. (B) Summation scores of Z-standardized T-cell signature genes stratified by median *JARID2* mRNA. (C) Summation scores of Z-standardized MHC-II signature genes stratified by median *JARID2* mRNA. (D) Z-standardized *JARID2* mRNA stratified by tumor-specific (IHC) HLA-DR status using a defined 5% cut-off. (E–G) *JARID2* mRNA expression z-scores in responders (complete response/partial response) compared with non-responders (progressive disease/stable disease) in patients given anti-PD-1. Mann-Whitney tests,  $*p \leq 0.05$ . *CIITA*, class II major histocompatibility complex transactivator II; *CTLA-4*, cytotoxic T-lymphocyte-associated protein 4; *EZH2*, enhancer of zeste 2 polycomb repressive complex 2 subunit; *HLA-DR*, human leukocyte antigen-DR; IHC, immunohistochemistry; *JARID2*, Jumoni and AT-rich interaction domain-containing protein; MHC, major histocompatibility complexes; mRNA, messenger RNA; PD-1, programmed death-1; PRC2, polycomb repressive complex 2.

However, some hypotheses for the utility of non-pAPCs to express MHC-II include potential priming via extracellular vesicles or exosomes,<sup>42</sup> or as a peripheral tolerance

mechanism to suppress T-cell responses via binding to LAG3 on activated lymphocytes.<sup>11</sup> Insights into the mechanism



for MHC-II expression in non-pAPCs may provide a better understanding for its role as a clinical predictor.

Despite multiple studies validating the role of MHC-II as a predictive biomarker, the functional role of MHC-II in response to PD-1/L1 targeted therapies requires further investigation. Reports from our laboratory<sup>43</sup> and others suggest it may have a functional role in response to PD-1/L1 therapies and this could be context dependent.<sup>15 16 44</sup> In this study we found that the PRC2 pathway plays a role in suppressing *CITTA*, and consequentially MHC-II expression. Treatment with the Food and Drug Administration (FDA)-approved EZH2 inhibitor tazemetostat can reverse PRC2 suppression and restore IFN-induced stimulation of MHC-II expression. In the current setting, MHC-II induction may function as a biomarker and be reflective of the overall response to IFN pathways, which are needed for immunotherapy responsiveness and have been known to be reprogrammed during chronic activation.<sup>45</sup> Thus, EZH2 inhibition may be a therapeutic strategy to reverse this cell state, leading to functional immunologic responses, and the data presented in this study supports clinical evaluation of EZH2 inhibition to overcome PD-1/L1 resistance.

It is not entirely clear why the PRC2 pathway plays a central role in MHC-II suppression. Prior studies performed in our laboratory demonstrated that in breast cancer MHC-I induction downstream of IFN stimulation is frequently suppressed by DNA methylation, and treatment with next-generation DNA methyltransferase inhibitors could reverse this phenotype.<sup>46</sup> Interestingly, in this previous study a concordant upregulation in MHC-II was not observed. Thus, the potential epigenetic pathways leading to suppression of MHC-I and MHC-II may be diverse or pathway-specific. Importantly, DNA methyltransferase and EZH2 inhibition were not evaluated head-to-head in either study, and a more comprehensive epigenetic study including multiple pathway inhibitors across cell lines and tumor types could be informative. Furthermore, it should be noted that the effects of epigenetic inhibitors are widespread and not confined to the *CITTA* locus. Therefore, additional studies will need to test the impact of EZH2 inhibition on antitumor immunity; such studies have been reported in an MHC-II agnostic manner.<sup>47</sup> Studies involving the genetic manipulation of MHC-II in preclinical models will be of particular interest in the establishment of an MHC-II-dependent connection between EZH2 inhibition and response to PD-1/L1 targeted therapies. Furthermore, previous studies have proposed EZH2 inhibition promotes antitumor immunity through a variety of mechanisms and require additional studies to dissect the potential contribution of upregulation of MHC-II to this effect.<sup>48</sup>

Given that tazemetostat is an FDA approved cancer therapy in other indications, these data support the experimental role of EZH2 inhibitors, like tazemetostat, potentially in combination with immunotherapy in anti-PD-1 resistant melanoma. Such approaches should incorporate biomarkers, such as PRC2 activity and/or pathway

expression, as well as dynamic on therapy biomarkers to determine what, if any, potential markers exist to identify patients most likely to benefit.

Overall, this study identifies PRC2 as a mediator of IFN-responsive MHC-II induction in melanoma cells and links this pathway to tumor inflammation. Understanding these relationships may elucidate the use of MHC-II as a predictive biomarker for clinical response to immunotherapies. Moreover, we independently identified and validated EZH2 as a mediator of MHC-II expression capacity consistent with prior findings,<sup>18 49 50</sup> and demonstrated broader connections to immunologic phenotype in tumors, clinical outcome, and potential for therapeutic intervention.

#### Author affiliations

<sup>1</sup>Department of Medicine, Vanderbilt University Medical Center, Nashville, Tennessee, USA

<sup>2</sup>Department of Medicine, Washington University in St Louis, St Louis, Missouri, USA

<sup>3</sup>Department of Biochemistry, Vanderbilt University, Nashville, Tennessee, USA

<sup>4</sup>Breast Cancer Research Program, Vanderbilt University Medical Center, Nashville, Tennessee, USA

<sup>5</sup>Department of Biostatistics, Vanderbilt University Medical Center, Nashville, Tennessee, USA

<sup>6</sup>Hematology/Oncology, Vanderbilt University Medical Center, Nashville, Tennessee, USA

<sup>7</sup>Department of Pathology, Microbiology, and Immunology, Vanderbilt University Medical Center, Nashville, Tennessee, USA

<sup>8</sup>Genetics Institute, Vanderbilt University, Nashville, Tennessee, USA

**Correction notice** This article has been corrected since it was first published online. Jamaal L James and Brandie C Taylor have now been listed as co-first authors and Catherine C Fahey has had their middle initial added.

**Twitter** Brandie C Taylor @bct255, Catherine C Fahey @catherine\_fahey and Justin M Balko @balkolab

**Acknowledgements** The authors would like to acknowledge and thank the members of the Vanderbilt SWERV writing core for the editing and development of this manuscript.

**Contributors** J.L.J., B.C.T., and J.M.B.: acquisition of data, analysis of data, and manuscript writing. M.L.A., L.N.G., P.I.G.-E., Y.W., V.S., E.H., and X.S.: acquisition of the data and analysis of the data. M.E.S. and D.B.J.: provision of the patient data, analysis of the data, and interpretation of the results. C.F.: revision of the manuscript for intellectual content. Y.X.: oversight of biostatistics and bioinformatics. J.M.B.: responsible for the overall content as the guarantor.

**Funding** This work was supported by NIH/NCI F30CA236157 (MLA) NIH T32GM007347 (MLA), NIH/NCI T32CA009592 (BCT), Susan G. Komen for the Cure 231038783 (BCT and JMB), NIH/NCI P30 CA068485 (JMB), NIH/NCI T32CA217834 (CF).

**Competing interests** MLA is listed as a co-inventor on a provisional patent application for methods to predict therapeutic outcomes using blood-based gene expression patterns, which is owned by Vanderbilt University Medical Center, and is currently unlicensed. D.B.J. has served on advisory boards or as a consultant for BMS, Catalyst Biopharma, lovance, Jansen, Mallinckrodt, Merck, Mosaic ImmunoEngineering, Novartis, Oncosec, Pfizer, Targovax, and Teiko, and has received research funding from BMS and Incyte. J.M.B. receives research support from Genentech/Roche, Bristol Myers Squibb, and Incyte Corporation, has received consulting/expert witness fees from Novartis, and is an inventor on provisional patents regarding immunotherapy targets and biomarkers in cancer. All other authors declare no potential conflicts of interest.

**Patient consent for publication** Not applicable.

**Ethics approval** Not applicable.

**Provenance and peer review** Not commissioned; externally peer reviewed.

**Data availability statement** Data are available upon reasonable request. Data are available upon request. De-identified metadata and RNAseq data from patients

with PD-1-treated melanoma is available at: <https://prod.tbilab.org/connect/#/apps/09ee3212-13fa-4c6b-ab87-73b0a84f2072/access>. Please contact the corresponding author ([justin.balko@vumc.org](mailto:justin.balko@vumc.org)) for an authorization key.

**Open access** This is an open access article distributed in accordance with the Creative Commons Attribution Non Commercial (CC BY-NC 4.0) license, which permits others to distribute, remix, adapt, build upon this work non-commercially, and license their derivative works on different terms, provided the original work is properly cited, appropriate credit is given, any changes made indicated, and the use is non-commercial. See <http://creativecommons.org/licenses/by-nc/4.0/>.

#### ORCID iDs

Brandie C Taylor <http://orcid.org/0000-0002-4862-4678>

Catherine C Fahey <http://orcid.org/0000-0003-4347-361X>

Justin M Balko <http://orcid.org/0000-0002-4263-5974>

#### REFERENCES

- Robert C, Schachter J, Long GV, *et al*. Pembrolizumab versus Ipilimumab in advanced Melanoma. *N Engl J Med* 2015;372:2521–32.
- Axelrod ML, Johnson DB, Balko JM. Emerging biomarkers for cancer Immunotherapy in Melanoma. *Semin Cancer Biol* 2018;52:207–15.
- Arlauckas SP, Garris CS, Kohler RH, *et al*. In vivo imaging reveals a tumor-associated macrophage-mediated resistance pathway in anti-PD-1 therapy. *Sci Transl Med* 2017;9:eaal3604.
- Marabelle A, Fakih M, Lopez J, *et al*. Association of tumour mutational burden with outcomes in patients with advanced solid tumours treated with Pembrolizumab: prospective biomarker analysis of the Multicohort, open-label, phase 2 KEYNOTE-158 study. *Lancet Oncol* 2020;21:1353–65.
- Meyer C, Cagnon L, Costa-Nunes CM, *et al*. Frequencies of circulating MDSC correlate with clinical outcome of Melanoma patients treated with Ipilimumab. *Cancer Immunol Immunother* 2014;63:247–57.
- Sade-Feldman M, Jiao YJ, Chen JH, *et al*. Resistance to Checkpoint blockade therapy through inactivation of antigen presentation. *Nat Commun* 2017;8:1136.
- Yarchoan M, Hopkins A, Jaffee EM. Tumor mutational burden and response rate to PD-1 inhibition. *N Engl J Med* 2017;377:2500–1.
- Zaretsky JM, Garcia-Diaz A, Shin DS, *et al*. Mutations associated with acquired resistance to PD-1 blockade in Melanoma. *N Engl J Med* 2016;375:819–29.
- Bernsen MR, Håkansson L, Gustafsson B, *et al*. On the biological relevance of MHC class II and B7 expression by tumour cells in Melanoma metastases. *Br J Cancer* 2003;88:424–31.
- Johnson DB, Estrada MV, Salgado R, *et al*. Melanoma-specific MHC-II expression represents a tumour-autonomous phenotype and predicts response to anti-PD-1/PD-L1 therapy. *Nat Commun* 2016;7:10582.
- Johnson DB, Nixon MJ, Wang Y, *et al*. Tumor-specific MHC-II expression drives a unique pattern of resistance to Immunotherapy via LAG-3/Fcrl6 engagement. *JCI Insight* 2018;3:e120360.
- Rodrig SJ, Gusenleitner D, Jackson DG, *et al*. MHC proteins confer differential sensitivity to CTLA-4 and PD-1 blockade in untreated metastatic Melanoma. *Sci Transl Med* 2018;10:eaar3342.
- Roemer MGM, Redd RA, Cader FZ, *et al*. Major Histocompatibility complex class II and programmed death ligand 1 expression predict outcome after programmed death 1 blockade in classic Hodgkin lymphoma. *J Clin Oncol* 2018;36:942–50.
- Gonzalez-Ericsson PI, Wulfkhule JD, Gallagher RI, *et al*. Tumor-specific major Histocompatibility-II expression predicts benefit to anti-PD-1/L1 therapy in patients with Her2-negative primary breast cancer. *Clin Cancer Res* 2021;27:5299–306.
- Bou Nasser Eddine F, Forlani G, Lombardo L, *et al*. CIITA-driven MHC class II expressing tumor cells can efficiently prime naive Cd4(+) TH cells in vivo and vaccinate the host against parental MHC-II-negative tumor cells. *Oncoimmunology* 2017;6:e1261777.
- Meazza R, Comes A, Orengo AM, *et al*. Tumor rejection by gene transfer of the MHC class II Transactivator in murine Mammary adenocarcinoma cells. *Eur J Immunol* 2003;33:1183–92.
- van Eggermond M, Boom DR, Klous P, *et al*. Epigenetic regulation of CIITA expression in human T-cells. *Biochem Pharmacol* 2011;82:1430–7.
- Truax AD, Thakkar M, Greer SF. Dysregulated recruitment of the Histone methyltransferase Ezh2 to the class II Transactivator (CIITA) promoter IV in breast cancer cells. *PLoS One* 2012;7:e36013.
- Kim KH, Roberts CWM. Targeting Ezh2 in cancer. *Nat Med* 2016;22:128–34.
- Ni Z, Abou El Hassan M, Xu Z, *et al*. The Chromatin-remodeling enzyme Brg1 coordinates CIITA induction through many interdependent distal enhancers. *Nat Immunol* 2008;9:785–93.
- Abou El Hassan M, Yu T, Song L, *et al*. Polycomb repressive complex 2 confers Brg1 dependency on the CIITA locus. *J Immunol* 2015;194:5007–13.
- Cerami E, Gao J, Dogrusoz U, *et al*. The cBio cancer Genomics portal: an open platform for exploring multidimensional cancer Genomics data. *Cancer Discov* 2012;2:401–4.
- Gao J, Aksoy BA, Dogrusoz U, *et al*. Integrative analysis of complex cancer Genomics and clinical profiles using the cBioPortal. *Sci Signal* 2013;6:pl1.
- Gu Z, Eils R, Schlesner M. Complex Heatmaps reveal patterns and correlations in multidimensional Genomic data. *Bioinformatics* 2016;32:2847–9.
- Burr ML, Sparbier CE, Chan KL, *et al*. An Evolutionarily conserved function of Polycomb silences the MHC class I antigen presentation pathway and enables immune evasion in cancer. *Cancer Cell* 2019;36:385–401.
- Xiao G, Jin L-L, Liu C-Q, *et al*. Ezh2 negatively regulates PD-L1 expression in hepatocellular carcinoma. *J Immunother Cancer* 2019;7:300.
- Wright KL, Ting J-Y. Epigenetic regulation of MHC-II and CIITA genes. *Trends Immunol* 2006;27:405–12.
- Muhlethaler-Mottet A, Di Bernardino W, Otten LA, *et al*. Activation of the MHC class II Transactivator CIITA by interferon-gamma requires cooperative interaction between Stat1 and USF-1. *Immunity* 1998;8:157–66.
- Leon Machado JA, Steimle V. The MHC class II Transactivator CIITA: not (quite) the odd-one-out anymore among NLR proteins. *Int J Mol Sci* 2021;22:1074.
- El-Jawahri A, LeBlanc T, VanDusen H, *et al*. Effect of inpatient palliative care on quality of life 2 weeks after hematopoietic stem cell transplantation: A randomized clinical trial. *JAMA* 2016;316:2094–103.
- Riaz N, Havel JJ, Makarov V, *et al*. Tumor and Microenvironment evolution during Immunotherapy with Nivolumab. *Cell* 2017;171:934–49.
- Axelrod ML, Cook RS, Johnson DB, *et al*. Biological consequences of MHC-II expression by tumor cells in cancer. *Clin Cancer Res* 2019;25:2392–402.
- Shi B, Vinyals A, Alia P, *et al*. Differential expression of MHC class II molecules in highly metastatic breast cancer cells is mediated by the regulation of the CIITA transcription implication of CIITA in tumor and metastasis development. *Int J Biochem Cell Biol* 2006;38:544–62.
- Holling TM, van Eggermond M, Jager MJ, *et al*. Epigenetic silencing of Mhc2Ta transcription in cancer. *Biochem Pharmacol* 2006;72:1570–6.
- Todd I, Pujol-Borrell R, Bottazzo GF, *et al*. Epithelial MHC class II sub-region expression in Autoimmunity. *Immunol Today* 1986;7:6.
- Londei M, Lamb JR, Bottazzo GF, *et al*. Epithelial cells expressing aberrant MHC class II determinants can present antigen to Cloned human T cells. *Nature* 1984;312:639–41.
- Wosen JE, Mukhopadhyay D, Macaubas C, *et al*. Epithelial MHC class II expression and its role in antigen presentation in the gastrointestinal and respiratory tracts. *Front Immunol* 2018;9:2144.
- Tsujiisaki M, Igarashi M, Sakaguchi K, *et al*. Immunochemical and functional analysis of HLA class II antigens induced by recombinant immune interferon on normal Epidermal Melanocytes. *J Immunol* 1987;138:1310–6.
- Deffrennes V, Vedrenne J, Stolzenberg MC, *et al*. Constitutive expression of MHC class II genes in Melanoma cell lines results from the transcription of class II Transactivator abnormally initiated from its B cell-specific promoter. *J Immunol* 2001;167:98–106.
- Roche PA, Furuta K. The INS and outs of MHC class II-mediated antigen processing and presentation. *Nat Rev Immunol* 2015;15:203–16.
- Duffy EB, Drake JR, Harton JA. Evolving insights for MHC class II antigen processing and presentation in health and disease. *Curr Pharmacol Rep* 2017;3:213–20.
- Van Niel G, Malleol J, Bevilacqua C, *et al*. Intestinal epithelial Exosomes carry MHC class II/peptides able to inform the immune system in mice. *Gut* 2003;52:1690–7.
- Balko JM, Johnson DB, Wang DY, *et al*. MHC-II expression to drive a unique pattern of adaptive resistance to antitumor immunity through receptor Checkpoint engagement. *JCO* 2018;36:180.
- Mortara L, Castellani P, Meazza R, *et al*. CIITA-induced MHC class II expression in Mammary adenocarcinoma leads to a Th1 polarization of the tumor Microenvironment, tumor rejection, and specific antitumor memory. *Clin Cancer Res* 2006;12:3435–43.





- 45 Kim YJ, Sheu KM, Tsoi J, *et al.* Melanoma Dedifferentiation induced by IFN- $\gamma$  epigenetic remodeling in response to anti-PD-1 therapy. *J Clin Invest* 2021;131:e145859.
- 46 Luo N, Nixon MJ, Gonzalez-Ericsson PI, *et al.* DNA methyltransferase inhibition Upregulates MHC-I to potentiate cytotoxic T lymphocyte responses in breast cancer. *Nat Commun* 2018;9:248.
- 47 Shin DS, Park K, Garon E, *et al.* Targeting Ezh2 to overcome the resistance to Immunotherapy in lung cancer. *Semin Oncol* 2022:S0093-7754(22)00045-8.
- 48 Wang D, Quiros J, Mahuron K, *et al.* Targeting Ezh2 Reprograms Intratumoral regulatory T cells to enhance cancer immunity. *Cell Rep* 2018;23:3262–74.
- 49 Mehta NT, Truax AD, Boyd NH, *et al.* Early epigenetic events regulate the adaptive immune response gene CIITA. *Epigenetics* 2011;6:516–25.
- 50 Boyd NH, Morgan JE, Greer SF. Polycomb recruitment at the class II Transactivator gene. *Mol Immunol* 2015;67:482–91.